Journal of the Korean Institute of Industrial Engineers
Vol. 34, No. 2, pp. 122-139, June 2008.

Performance and Robustness of Control Charting Methods for Autocorrelated Data

Chang-Ho Chin[1†] · Daniel W. Apley[2]

[1]School of Mechanical and Industrial Systems Engineering, Kyung Hee University, Yongin 446-701, Korea
[2]Department of Industrial Engineering and Management Sciences, Northwestern University, USA

With the proliferation of in-process measurement technology, autocorrelated data are increasingly common in industrial SPC applications. A number of high performance control charting techniques that take into account the specific characteristics of the autocorrelation through time series modeling have been proposed over the past decade. We present a survey of such methods and analyze and compare their performances for a range of typical autocorrelated process models. One practical concern with these methods is that their performances are often strongly affected by errors in the time series models used to represent the autocorrelation. We also provide some analytical results comparing the robustness of the various methods with respect to time series modeling errors.

***Keywords*: Control Charts, Autocorrelation, Robustness, Average Run Length, Sensitivity Measure**

1. Introduction

Statistical process control (SPC) has been used to achieve and maintain control of various processes in industry (Stoumbos, Reynolds, Ryan, and Woodall 2000). The control chart is a primary SPC tool to monitor process variability and promote quality improvement by means of detecting process shifts requiring corrective actions. As a graphical monitor, control charts generally contain a centerline and two other horizontal lines called control limits, the width of which is often proportional to the standard deviation of the charted statistic. If a point plots outside the control limits, the process is declared not to be in a state of control.

Since the advent of Shewhart charts, many control charts have been developed to monitor, control, and improve processes. Traditional control charts such as x-bar charts, CUSUM (cumulative sum) charts, and exponentially weighted moving average (EWMA) charts assume the independence of observations over time. With significant advances in measurement and data collection technology, however, measurements are taken at increasingly higher rates and are more likely to be autocorrelated (Montgomery and Woodall 1997; Woodall and Montgomery 1999). This leads to a significant deterioration of traditional control chart performance, a phenomenon that has been discussed by Johnson and Bagshaw (1974), Bagshaw and Johnson (1975), Harris and Ross (1991), Alwan (1992), Woodall and Faltin (1993), and many others. Positive autocorrelation typically increases the variance of the charted statistic so that the control limits determined under the independence assumption are too narrow, giving a higher-than-expected number of false alarms. Goldsmith and Whitefield (1961) revealed this relation between the nature of autocorrelation and the false alarm rate for CUSUM charts.

There are two primary classes of approaches for control charting in the presence of autocorrelation: Applying traditional control charts to the original autocorrelated data with the control limits adjusted to account

This research is supported by the Kyung Hee University Research Fund in 2005. (KHU-20051078).
† Corresponding author : Chang-Ho Chin, School of Mechanical and Industrial Systems Engineering, Kyung Hee University, Yongin-si, Gyeonggi-do 446-701, Korea. Fax. +82-31-203-4004, E-mail: chin@khu.ac.kr
Received March 2007; revision received April 2008; accepted May 2008.

for the autocorrelation (Johnson and Bagshaw 1974; Vasilopoulos and Stamboulis 1978; Yashchin 1993; Wardell, Moskowitz, and Plante 1994; VanBrackle and Reynolds 1997; Zhang 1998) and fitting a time-series model to the process data and applying control charts to the uncorrelated residuals of the model with normal control limits (Alwan and Roberts 1988 Wardell, Moskowitz, and Plante 1992; Runger, Willemain, and Prabhu 1995; Lin and Adams 1996; Apley and Shi 1999). Moreover, many control charting techniques in the second category are designed to take into account the specific characteristics of the autocorrelation through time series modeling (e.g., Box and Ramírez 1992; Luceño 1999; Apley and Shi 1999; Chin and Apley 2006; Apley and Chin 2007).

In light of the fact that effective methods for control charting autocorrelated processes are of increasing importance as data-rich environments such as in manufacturing and service industries proliferate, this paper surveys various methods and investigates their relative performance and robustness. Here, robustness is with respect to errors in the fitted time series models that are used to represent the autocorrelation. Many of the papers just cited have noted that lack of robustness to modeling errors is one of the most serious shortcomings of control charts for autocorrelated data. Although for the performance comparison we primarily rely on simulation, for the robustness comparison we develop analytical results that provide insight into why some charts are robust but others are not.

The format of the remainder of the paper is as follows. Section 2 presents a survey of control charting techniques for autocorrelated data. In Section 3, the performances of such methods are compared for a variety of autocorrelated processes that can be represented as autoregressive moving average (ARMA) time series models. We derive some analytical robustness results in Section 4 and verify these with simulation in Section 4. Section 5 concludes the paper.

2. Survey of Control Charting Methods for Autocorrelated Data

Through this paper, the process data x_t (t is a time index or observation number) is assumed to follow an ARMA process model, plus (potentially) an additive deterministic mean shift, μ_t, the form of which is (Box, Jenkins, and Reinsel 1994)

$$x_t = \frac{\Theta(B)}{\Phi(B)} a_t + \mu_t,$$

where B is the time-series backward shift operator defined such that $Bx_t = x_{t-1}$; a_t is an independently and identically distributed (i.i.d.) Gaussian process with mean 0 and variance σ_a^2 denoted $a_t \sim NID(0, \sigma_a^2)$; $\Phi(B) = (1 - \phi_1 B - \phi_2 B^2 - \cdots - \phi_p B^p)$ and $\Theta(B) = (1 - \theta_1 B - \theta_2 B^2 - \cdots - \theta_q B^q)$ are the AR and MA polynomials of order p and q, respectively. $\mu_t = 0$ for all t for the in-control process and $\mu_t \neq 0$ for the out-of-control process. We are assuming, without loss of generality, that the in-control mean is zero. The model residuals (i.e., the one-step-ahead prediction errors) are generated via the linear filtering operation (Apley and Shi 1999).

$$e_t = \frac{\Phi(B)}{\Theta(B)} x_t = \frac{\Phi(B)}{\Theta(B)} \left[\frac{\Theta(B)}{\Phi(B)} a_t + \mu_t \right] \qquad (1)$$

$$= a_t + \frac{\Phi(B)}{\Theta(B)} \mu_t = a_t + \widetilde{\mu_t},$$

where $\widetilde{\mu_t} = \Phi(B)/\Theta(B)\mu_t$ is a filtered version of the deterministic mean shift μ_t. The residuals are uncorrelated under the assumption that the fitted model used to generate the residuals is a perfect representation of reality. Because this is never the case in practice, a later section of this paper is devoted to quantifying the effect of modeling errors on the performance of the charts. For the time being, however, we assume that there are no modeling errors.

2.1 Conventional Methods Modified for Autocorrelated Data

In this section, we review Shewhart, CUSUM (cumulative sum), and EWMA charts applied either to the autocorrelated data with control limits modified to take into account the autocorrelation or to the residuals e_t.

Vasilopoulos and Stamboulis (1978) proposed modified control limits for an x-bar chart and an s chart for autocorrelated data x_t that follow a second-order autoregressive [AR(2)] model with a constant mean shift μ

$$x_t = \frac{1}{\left(1 - \phi_1 B - \phi_2 B^2\right)} a_t + \mu,$$

The $L\sigma$ control limits on $\overline{x}$ are given by

$$\pm \lambda^{1/2}(\phi_1, \phi_2, n) L\sigma_a / \sqrt{n}, \tag{2}$$

where n is the subgroup size and $\lambda^{1/2}(\phi_1, \phi_2, n)$ is a correction factor that widens/narrows the control limits to take into account the autocorrelation (see the Appendix of Vasilopoulos and Stamboulis (1978) for specific values). The constant L is chosen to provide a desired in-control average run length (ARL) or a false alarm rate. In the case of no serial correlation so that $\phi_1 = 0$ and $\phi_2 = 0$, the $\lambda^{1/2}(\phi_1, \phi_2, n) = 1$, and the control limits reduce to the traditional $\pm L\sigma$ control limits. For example, 3σ control limits on uncorrelated data give an in-control ARL of 370. As an example of autocorrelated data, suppose that $\phi_1 = 1.2$ and $\phi_2 = -0.4$. In this case, the adjusted 3σ control limits for subgroups of size $n = 5$ are $\pm 2.53\sigma_a$, while the traditional control limits $\pm 1.342\sigma_a$ are much narrower and would result in many false alarms.

Johnson and Bagshaw (1974) established a theoretical basis for obtaining approximate thresholds h of one-sided CUSUM charts to provide desired performances for autocorrelated data. They considered the one-sided CUSUM chart proposed by Page (1955) with a test statistic $C_i = \max[0, x_i - K + C_{i-1}]$ for observations x_i, where $E(x_i) = 0$, $\mathrm{Var}(x_i) = \sigma_x^2 < \infty$, and K is a reference value. For autocorrelated AR(1) and MA(1) processes, the run length distribution and its ARL ($\approx h^2/\sigma_x^2$) were approximated by establishing the convergence of the normalized partial sums to a Wiener process and using the usual Wiener process approximation. The threshold h were defined with the estimate of the standard deviation σ_x and a threshold h_I which is based on the assumption of zero correlation and unit variance for the observations. If the estimate of the standard deviation, $\Sigma(x_i - \bar{x})^2/n$, is used for AR(1) autocorrelated data $x_1, x_2, x_3, \cdots, x_n$, the threshold h becomes $h_I\sigma_a\sqrt{(1-\phi_1^2)^{-1}}$ and the corresponding ARL $\doteq \frac{h^2}{\sigma_x^2} = \frac{h_I^2\sigma_a^2(1-\phi_1^2)^{-1}}{\sigma_a^2(1-\phi_1)^{-2}} = h_I^2\frac{(1-\phi_1)}{(1+\phi_1)}$. Johnson and Bagshaw (1974) derived some approximate formula for modifying (usually widening) the control limits to take into account the autocorrelation. The correction factor is a function of the parameters of the ARMA model used to represent the autocorrelation.

Zhang (1998) proposed the EWMAST chart, an EWMA chart for stationary processes, in which the charted statistic is the EWMA statistic introduced by Roberts (1959)

$$z_t = (1-\lambda)z_{t-1} + \lambda x_t, \tag{3}$$

where $z_0 = 0$, and λ is a constant ($0 < \lambda \leq 1$). The difference between the EWMAST and the conventional EWMA chart is that the variance of EWMA statistic z_t, upon which the control limits are based, is calculated using the autocorrelation function of x_t (denoted by $\rho(k)$ for lag $k = 1, 2, 3, \cdots$):

$$\sigma_z^2 = \mathrm{var}[z_t] = \sigma_x^2[\lambda/(2-\lambda)] \tag{4}$$
$$\left\{1-(1-\lambda)^{2t} + 2\Sigma_{k=1}^{t-1}\rho(k)(1-\lambda)^k[1-(1-\lambda)^{2(t-k)}]\right\}.$$

This reduces to the conventional EWMA variance (see Hunter, 1986), when no autocorrelation exists in the data (i.e., $\rho(k) = 0$). As for the aforementioned Shewhart and CUSUM charts, the control limits for the EWMAST chart are also established based on the variance of chart statistic, taking into account the autocorrelation. The objective is to provide a desired false alarm rate of in-control ARL.

Traditional control charts also can be applied directly to the model residuals in Equation (1) without any modification of the control limits, as long as the process model is accurate, in which case the residuals are uncorrelated. One common example of residual-based control charts is an EWMA control chart on the residuals, which is of the form $y_t = (1-\lambda)y_{t-1} + \lambda e_t$ with control limits $\pm L\sigma_y$, where $\sigma_y = (\lambda/(2-\lambda))^{1/2}\sigma_a$ equals the steady-state (large t) version of σ_z in Equation (4) when there is no autocorrelation. This control charting scheme provides the same ARL as an EWMA control chart on independent observations x_t with control limits $\pm L(\lambda/(2-\lambda))^{1/2}\sigma_x$. Another version of residual-based control charting scheme proposed by Jiang *et al.* (2002) is monitoring residuals obtained by subtracting the proportional integral derivative (PID) predictor from the original process data: $e_t = x_t - \hat{x}_t$. Residual-based control charts have been broadly investigated (Berthouex, Hunter, and Pallesen 1978, Alwan and Roberts 1988, Montgomery and Mastrangelo 1991, Superville and Adams 1994, Wardell, Moskowitz, and Plante 1994, Runger, Willemain, and Prabhu 1995, Lin and Adams, 1996, Vander Wiel 1996, Apley and Shi 1999, Lu and Reynolds 1999a, English, Lee, Martin, and Tilmon 2000).

2.2 Methods Developed for Autocorrelated Data

Equation (1) implies that e_t is composed of random shock a_t and the filtered version of the deterministic mean shift μ_t. The $\tilde{\mu}_t$ component experiences certain dynamics that depend on the ARMA process model, after which it settles down to a steady-state value if the ARMA model is stable and invertible and μ_t is a step mean shift in the original process. To illustrate how a step mean shift in the original process can result in a time-varying mean shift in the residuals, consider the mechanical vibratory system of Pandit and Wu (1983), an ARMA(2,1) model for which is given by (Jiang *et al.* 2000),

$$x_t = \frac{(1+0.519B)}{(1-1.439B+0.600B)}a_t + \mu_t$$

where $\sigma_a = 2.21$. For a step mean shift defined as $\mu_t = 2\sigma_a$ for $t > 0$ and 0, otherwise, the residual mean $\tilde{\mu}_t$ oscillates about zero as shown in <Figure 1>, before eventually converging to a small steady-state value. This property that any significant initial dynamics soon decay to a minor lasting effect on the residuals has been referred to as forecast recovery (Superville and Adams 1994; Apley and Shi 1999). Forecast recovery is detrimental to the detection performance of traditional control charts.

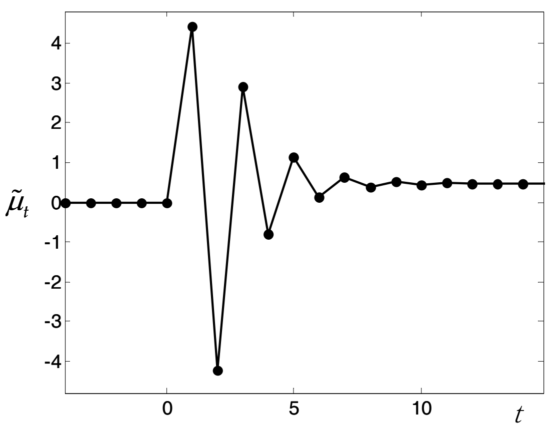

Figure 1. Residual Mean

In order to improve the charting performance in the face of forecast recovery, a number of residual-based control charts have been proposed that specifically look for the presence of the dynamics or "patterns" represented by $\tilde{\mu}_t$ in the residuals. Such charts include the CUSCORE (Fisher 1925, Bagshaw and Johnson 1977, Box and Ramírez 1992, Box and Luceño 1997, Luceño 1999), the GLRT (Apley and Shi 1999), the optimal general linear filter (OGLF, Apley and Chin 2007), and the optimal second-order linear filter (OSLF, Chin and Apley 2006).

One of the various CUSCORE Charts based on the efficient score statistics of Fisher (1925) was proposed by Luceño (1999) and analyzed by Shu, Apley, and Tsung (2002), Runger and Testik (2003), and Luceño (2004). The upper one-sided CUSCORE is calculated recursively via

$$S_t = \max[\{S_{t-1} + (e_t - \tilde{\mu}_t/2)\tilde{\mu}_t\};0] \tag{5}$$

and sounds an alarm when S_t exceeds a pre-specified threshold. The GLRT statistic of Apley and Shi (1999) based on a likelihood ratio test also uses a feared residual mean shift as the amplifier

$$G(t) \equiv \max_{\xi=1,\cdots,N} \left|T_\xi(t)\right|,$$

where $T_\xi(t) = \left(\sigma_a^2 \sum_{j=1}^{\xi} \tilde{\mu}_j^2\right)^{-1/2} \sum_{j=1}^{\xi} e_{t-\xi+j}\tilde{\mu}_j$. (6)

The GLRT statistic tests for mean shifts occurring at each time $t - \xi + 1$ ($\xi = 1, 2, \cdots, N$) within a moving window of length N. $T_\xi(t)$ in Equation (6) can be considered as a measure of correlation between the residuals and a feared signal occurring at time $t - \xi + 1$. The higher the correlation, the more likely it is that a feared signal occurred at that specific time. The GLRT signals when $G(t)$ exceeds a pre-specified threshold h chosen to provide a desired in-control ARL. In situations that residual mean shift dynamics are pronounced (Apley and Shi 1999), the GLRT outperforms traditional control charts such as the Shewhart and CUSUM charts applied to the residuals which do not make use of the valuable information in the dynamics.

We can view the Equations (5) and (6) for generating the charted statistics as multiplying the residuals by a sequence of detector coefficients that are precisely the elements of $\tilde{\mu}_t$. The conceptual effect of this is to amplify the presence of $\tilde{\mu}_t$ in the residuals following a mean shift. Note that $\tilde{\mu}_t$ is sometimes called the feared signal, and the CUSCORE and GLRT are viewed as matched filters. The OGLF and OSLF have a similar intent, except that their coefficients are only

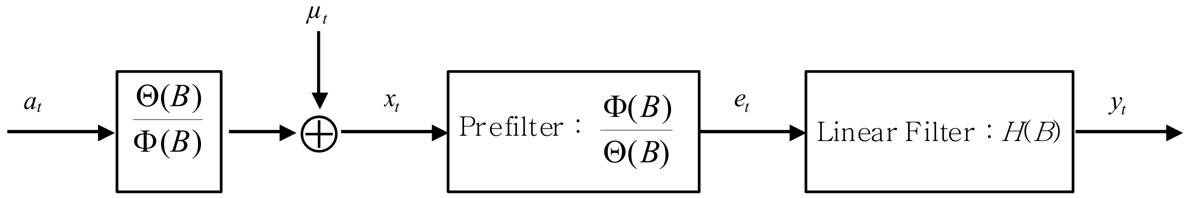

Figure 2. Block Diagram Representation of a Control Chart Statistic y_t Generated via a Linear Filtering peration.

based on $\tilde{\mu}_t$ and do not necessarily coincide with the elements of $\tilde{\mu}_t$.

The OGLF was developed recognizing that many common control charts can be viewed as charting the output of a linear filter applied to process data (Apley and Chin 2007). The statistics of many control charts such as the Shewhart and the EWMA charts applied to x_t can be represented in the form of $y_t = H(B)x_t$, where $H(B) = h_0 + h_1B + h_2B^2 + \cdots$ is some linear filter in impulse response form and $\{h_j : j = 0, 1, 2, \cdots\}$ are the impulse response coefficients of the filter (see Box, Jenkins, and Reinsel 1994 for basic background on linear filtering). For the EWMA in Equation (3), $z_t = H(B)x_t = (\lambda(1-(1-\lambda)B)^{-1})x_t = (\lambda + \lambda(1-\lambda)B + \lambda(1-\lambda)^2B^2 + \cdots)x_t$ and $h_j = \lambda(1-\lambda)^j$. The Shewhart individual chart with statistic $y_t = x_t$ has the identity filter, $H(B) = 1$ (see Apley and Chin (2007) for more examples). This generalization also applies to residual- based charts, where one can view the residual generation as a linear pre-filter $\Theta^{-1}(B)\Phi(B)$ applied to x_t, and then the filter $H(B)$ is applied to e_t. <Figure 2> depicts this graphically.

More specifically, the OGLF charted statistic proposed by Apley and Chin (2007) is of the form

$$y_t = H(B)e_t = \sum_{j=0}^{Tr} h_j e_{t-j}, \tag{7}$$

where *Tr* is a suitably large truncation time and control limits are fixed at ±1 because the filter coefficients can be scaled accordingly. A gradient-based filter optimization strategy was also proposed for directly determining the filter coefficients $\{h_j\}$ to minimize the out-of-control ARL (denoted by ARL_1) while constraining the in-control ARL (denoted by ARL_0) to some desired value. In this respect, the OGLF is automatically tuned to best detect the presence of $\tilde{\mu}_t$ in the residuals.

The OSLF chart of Chin and Apley (2006) is a special case of the OGLF defined such that $H(B)$ is restricted to the class of all second-order linear filters, which considerably simplifies its design and implementation. Specifically, the OSLF charted statistic is of the form

$$y_t = \gamma\left[\frac{1-\beta B}{1-\alpha_1 B - \alpha_2 B^2}\right]e_t, \tag{8}$$

where α_1, α_2, β, and γ are the OSLF design parameters to be determined and the control limits are ±1 due to the scaling constant γ. The design procedure of the OSLF uses the same ARL_1 optimization criterion and ARL_0 constraint as the OGLF. For certain autocorrelated processes with prominent residual mean dynamics, the OGLF and OSLF coefficients tends to mimic the shape characteristic of the residual mean. In many examples (Chin and Apley 2006), the OSLF performs substantially better than an optimized EWMA and almost as good as the OGLF.

3. Performance Analysis

3.1 Simulation Strategy

As discussed in Section 2, two primary methods to deal with the adverse effects of autocorrelation on control charts are adjusting the control limits according to the nature of the autocorrelation and control charting the residuals. For the latter, one can either apply standard control charts or control charts that are designed to detect the dynamics of the residual mean. For the performance comparison, we focus on residual-based control charts because they generally perform better, are more straightforward to design, and have more tractable ARL computation. Apley and Lee (2008) pointed out that the residual-based EWMA has a better performance/robustness tradeoff relative to an EWMA on x_t.

The performance of residual-based control charts de-

Table 1. Zero-state ARL Comparison for the OGLF, the OSLF, the CUSCORE, and the GLRT

	Tim Series Model		*Shift*		*OGLF*		*OSLF*		*OPtimal EWMA*		*CUSCORE*		*GLRT*	
No.	ϕ_1	θ_1	*Type*	*Size*	ARL$_0$zs	ARL$_1$zs	ARL$_0$zs	ARL$_1$zs	ARL$_0$zs	ARL$_1$zs	ARL$_0$zs	ARL$_1$zs	ARL$_0$zs	ARL$_1$zs
1	0	0	Step	0.5	499.24 (3.05)	**28.38** (0.10)	499.24 (3.05)	**28.38** (0.10)	499.24 (3.05)	**28.38** (0.10)	499.63 (3.18)	31.27 (0.11)	500.60 (3.11)	48.34 (0.26)
2	0	0	Step	1.5	500.81 (3.15)	**5.45** (0.02)	500.81 (3.15)	**5.45** (0.02)	500.81 (3.15)	**5.45** (0.02)	500.74 (3.17)	**5.45** (0.02)	500.12 (3.14)	5.66 (0.02)
3	0	0	Step	3	500.02 (3.14)	1.87 (0.01)	500.02 (3.14)	1.87 (0.01)	500.02 (3.14)	1.87 (0.01)	500.77 (3.16)	**1.79** (0.01)	500.83 (3.18)	1.92 (0.01)
4	0	0	Step	4	500.43 (3.16)	1.21 (0.00)	500.43 (3.16)	1.21 (0.00)	500.43 (3.16)	1.21 (0.00)	499.28 (3.15)	**1.20** (0.00)	500.78 (3.13)	1.31 (0.00)
5	0.9	0	Step	0.5	500.16 (2.71)	**353.79** (1.79)	500.16 (2.71)	**353.79** (1.79)	500.16 (2.71)	353.79 (1.79)	500.46 (2.62)	375.76 (1.88)	500.36 (3.14)	473.82 (2.96)
6	0.9	0	Step	1.5	500.37 (2.86)	**129.60** (0.57)	500.37 (2.86)	**129.60** (0.57)	500.37 (2.86)	129.60 (0.57)	499.01 (3.01)	138.02 (0.78)	500.48 (3.13)	324.75 (2.16)
7	0.9	0	Step	3	499.24 (3.03)	47.32 (0.31)	500.75 (3.07)	48.00 (0.32)	500.76 (3.00)	49.73 (0.22)	499.81 (3.11)	**30.99** (0.28)	500.64 (3.15)	78.77 (0.85)
8	0.9	0	Step	4	499.96 (3.11)	14.01 (0.18)	500.63 (3.10)	14.00 (0.18)	500.77 (3.06)	29.44 (0.14)	499.17 (3.08)	**8.04** (0.13)	500.64 (3.15)	14.92 (0.29)
9	0.9	0	Spike	0.5	499.14 (3.15)	**490.17** (3.12)	500.43 (3.14)	493.43 (3.11)	500.55 (3.17)	500.13 (3.15)			500.18 (3.18)	491.94 (3.11)
10	0.9	0	Spike	1.5	499.29 (3.14)	**418.03** (3.11)	499.20 (3.12)	424.69 (3.13)	499.34 (3.15)	454.13 (3.14)			499.95 (3.15)	433.78 (3.14)
11	0.9	0	Spike	3	499.98 (3.17)	**84.12** (1.76)	500.13 (3.14)	88.45 (1.81)	499.01 (3.15)	176.54 (2.38)			499.23 (3.12)	97.98 (1.87)
12	0.9	0	Spike	4	500.66 (3.13)	**6.25** (0.43)	499.62 (3.19)	7.00 (0.45)	500.76 (3.14)	27.85 (0.98)			500.70 (3.14)	8.41 (0.54)
13	0	0	Sinusoid	S_1	499.22 (3.09)	**15.78** (0.05)	499.22 (3.09)	**15.78** (0.05)	500.56 (3.14)	122.56 (1.31)	499.62 (3.15)	15.82 (0.06)	499.33 (3.14)	19.64 (0.09)
14	0	0	Sinusoid	S_2	499.51 (3.08)	**30.74** (0.11)	499.51 (3.08)	**30.74** (0.11)	500.63 (3.18)	225.55 (2.13)	500.12 (3.10)	31.04 (0.13)	500.15 (3.14)	46.59 (0.29)
15	0	0	Sinusoid	S_3	499.12 (3.07)	**33.34** (0.14)	500.17 (3.13)	43.47 (0.25)	499.44 (3.17)	177.91 (1.78)	499.50 (3.05)	33.86 (0.16)	500.84 (3.10)	48.45 (0.31)
16	0	0	Sinusoid	S_4	500.91 (3.10)	10.64 (0.04)	499.37 (3.11)	11.40 (0.04)	499.45 (3.16)	26.23 (0.16)	499.92 (3.13)	10.58 (0.04)	499.80 (3.16)	**10.54** (0.04)
17	0.9	-0.9	Step	0.5	499.80 (2.72)	446.77 (2.37)	499.80 (2.72)	446.77 (2.37)	499.80 (2.72)	446.77 (2.37)	499.61 (4.80)	**343.69** (3.70)	499.14 (3.14)	475.79 (3.10)
18	0.9	-0.9	Step	1.5	499.63 (2.93)	142.06 (1.73)	500.91 (3.10)	162.26 (2.21)	499.74 (2.73)	257.46 (1.24)	500.74 (3.97)	**86.56** (1.43)	499.37 (3.13)	193.75 (2.38)
19	0.9	-0.9	Step	2	500.86 (3.09)	41.78 (1.12)	500.03 (3.06)	42.21 (1.14)	500.93 (3.16)	194.06 (0.91)	500.01 (3.39)	**29.02** (0.77)	499.19 (3.12)	55.60 (1.36)
20	0.9	-0.9	Step	3	499.05 (3.09)	3.16 (0.08)	500.37 (3.17)	3.33 (0.13)	499.27 (3.14)	74.70 (1.53)	500.01 (3.14)	3.33 (0.19)	499.61 (3.15)	**2.43** (0.08)
21	0.9	0.5	Step	0.5	499.02 (2.73)	**206.73** (0.97)	500.13 (2.81)	206.91 (0.96)	500.13 (2.81)	206.91 (0.96)	500.25 (2.75)	235.32 (1.12)	500.13 (3.09)	398.64 (2.52)
22	0.9	0.5	Step	1.5	499.72 (3.00)	**50.82** (0.22)	499.72 (3.00)	**50.82** (0.22)	499.72 (3.00)	**50.82** (0.22)	499.15 (3.07)	54.34 (0.29)	500.95 (3.16)	113.86 (0.79)
23	0.9	0.5	Step	3	500.08 (3.12)	10.73 (0.08)	500.08 (3.12)	10.73 (0.08)	499.27 (3.11)	10.69 (0.08)	500.45 (3.11)	**6.88** (0.07)	500.11 (3.15)	7.96 (0.09)
24	0.9	0.5	Step	4	500.62 (3.15)	2.77 (0.03)	500.40 (3.12)	2.85 (0.04)	500.36 (3.14)	2.83 (0.04)	499.21 (3.16)	1.85 (0.03)	499.56 (3.15)	**1.68** (0.01)
25	0.9	0.5	Spike	0.5	499.70 (3.11)	497.13 (3.15)	499.46 (3.13)	497.88 (3.14)	500.83 (3.19)	499.58 (3.17)			499.30 (3.15)	496.52 (3.16)
26	0.9	0.5	Spike	1.5	499.55 (3.10)	**457.83** (3.08)	500.84 (3.17)	466.37 (3.14)	499.25 (3.17)	467.66 (3.13)			499.40 (3.15)	463.13 (3.13)
27	0.9	0.5	Spike	3	500.99 (3.13)	**207.74** (2.52)	500.57 (3.15)	258.83 (2.75)	499.10 (3.15)	260.10 (2.78)			499.41 (3.12)	213.92 (2.56)
28	0.9	0.5	Spike	4	500.47 (3.16)	**50.40** (1.30)	499.38 (3.17)	83.39 (1.75)	500.16 (3.19)	84.60 (1.76)			500.15 (3.14)	54.04 (1.45)
29	0	0	Ramp	0.5	499.18 (3.08)	**33.28** (0.11)	499.18 (3.08)	**33.28** (0.11)	499.83 (3.07)	33.33 (0.11)	500.09 (3.08)	35.94 (0.12)	499.88 (3.14)	59.15 (0.31)
30	0	0	Ramp	1.5	500.09 (3.12)	**10.50** (0.02)	500.09 (3.12)	**10.50** (0.02)	500.04 (3.14)	10.51 (0.02)	499.56 (3.11)	10.96 (0.02)	500.61 (3.11)	11.17 (0.02)
31	0	0	Ramp	3	500.82 (3.13)	**6.60** (0.01)	500.82 (3.13)	**6.60** (0.01)	499.78 (3.17)	**6.60** (0.01)	500.94 (3.16)	6.82 (0.01)	499.50 (3.14)	6.88 (0.01)
32	0	0	Ramp	4	499.16 (3.14)	**5.49** (0.01)	499.16 (3.14)	**5.49** (0.01)	500.84 (3.13)	5.50 (0.01)	500.54 (3.17)	5.64 (0.01)	500.12 (3.15)	5.74 (0.01)

pends strongly on the characteristics of the residual mean, which depend on the characteristics of the process as represented by the ARMA model and the form and magnitude of the mean shift. Thus, we consider a broad combination of scenarios in the 32 examples listed in <Table 1>. All processes for comparison are modeled as ARMA(1,1) plus possibly a deterministic mean shift

$$x_t = \frac{(1-\theta_1 B)}{(1-\phi_1 B)} a_t + \mu_t,$$

which includes, as special cases, AR(1) when $\theta_1 = 0$, MA(1) when $\phi_1 = 0$, and i.i.d. when $\phi_1 = \theta_1 = 0$. Without loss of generality, σ_a is assumed to be 1 for the remainder of the paper. Step, spike, sinusoidal, and ramp mean shifts are considered with a wide range of magnitudes from 0 to $4\sigma_a$. The step mean shift is defined as $\mu_t = 0$ for $t < 1$ and $\mu_t = \mu$ for $t \geq 1$ and the spike mean shift is defined as $\mu_1 = \mu$ and $\mu_t = 0$ for $t \neq 1$. The sinusoidal shifts are denoted S_1-S_4 in <Table 1>. S_1, S_2, and S_3 are sinusoidal functions with amplitude 0.75 and periods of 2, 4, and 8 timesteps, respectively. S_4 has amplitude 1.5 and period 8 timesteps. The ramp mean shift is defined as $\mu_t = 0$ for $t < 1$, $\mu_t = \mu t/10$ for $1 \leq t < 10$ and $\mu_t = \mu$ for $t \geq 10$. <Figure 3> shows the residual means of Examples 4, 8, 12, 16, 20, 24, 28, and 32. For different magnitude mean shifts, the residual means have exactly the same shapes but are scaled differently.

We compare EWMA, OGLF, OSLF, CUSCORE, and GLRT charts in terms of their ARL performance. The EWMA chart is one of the most popular control charting methods and is often recommended for monitoring the residuals of autocorrelated data. In fact, the EWMA chart is revealed to be optimal in several situations under consideration in this paper. Note that the EWMA reduces to a Shewhart individual chart in the limit (as λ approaches 1.0) such as in Examples 9~12 and 25~28, which is known to be effective at detecting spikes. Although it will be shown that the CUSCORE outperforms the EWMA for the examples in which the residual mean has pronounced dynamics, there are quite a few examples in which the EWMA outper-

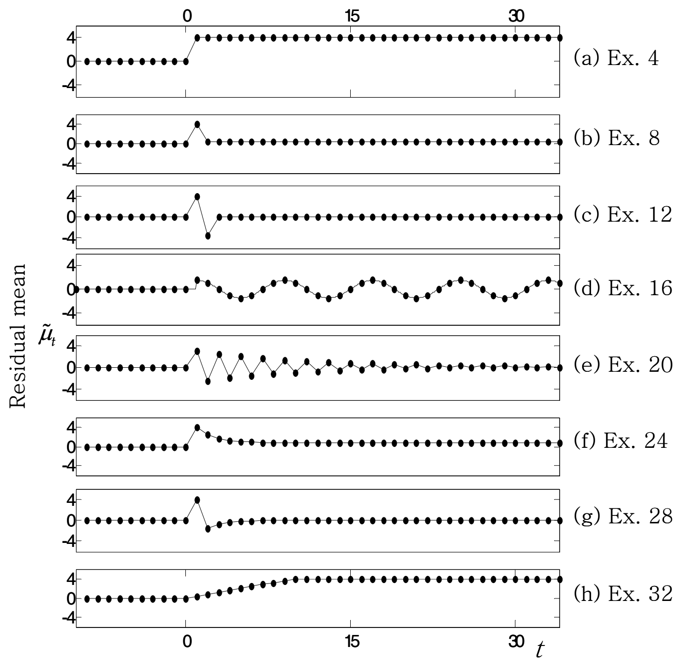

Figure 3. Illustration of residual mean shifts for ARMA(1, 1) processes : (a) i.i.d. process ($\phi_1 = \theta_1 = 0$) with a step mean shift of size 4; (b) AR(1) process ($\phi_1 = 0.9$) with a step mean shift of size 4; (c) AR(1) process ($\phi_1 = 0.9$) with a spike mean shift of size 4 (d) i.i.d. process ($\phi_1 = \theta_1 = 0$) with a sinusoidal mean shift of period 8 and amplitude 1.5; (e) ARMA(1,1) process ($\phi_1 = 0.9$, $\theta_1 = -0.9$) with a step mean shift of size 3; (f) ARMA(1,1) process ($\phi_1 = 0.9$, $\theta_1 = 0.5$) with a step mean shift of size 4; (g) ARMA(1,1) process ($\phi_1 = 0.9$, $\theta_1 = 0.5$) with a spike mean shift of size 4; (h) i.i.d. process ($\phi_1 = \theta_1 = 0$) with a ramp mean shift of size 4.

forms the CUSCORE or performs quite comparably to it (e.g., the common, practical scenarios of Examples 1~ 4 and 29~30, in which there is a sustained step and a drifting ramp shift in i.i.d. data). The PID chart is not included into the comparison. We had compared the PID chart to the OGLF and OSLF charts in Chin and Apley (2006) and Apley and Chin (2007) and found that when one used the design guidelines suggested by Jiang *et al.* (2002), the performance of the PID chart was not competitive with the other charts.

We calculated the zero-state ARL for each example based on Monte Carlo simulation with 25,000 replicates. The zero-state ARL refers to the ARL of which the evaluation starts with the initial observation. Because the EWMA, OGLF, and OSLF charts are inherently two-sided and the absolute value in Equation (6) makes the GLRT chart two-sided, the two-sided versions of the CUSCORE chart is considered for comparison. The lower-sided CUSCORE statistic would be constructed substituting -$\tilde{\mu}_t$ for $\tilde{\mu}_t$ in Equation (5), and the two-sided version consists of the two one-sided versions together. The CUSUM chart is not included in this comparison because the EWMA chart performance is virtually identical (Vander Wiel 1996, Yang and Makis 1997, Montgomery 2005). The residual- based EWMA chart for comparison is defined as

$$y_t = (1-\lambda)y_{t-1} + \zeta e_t, \tag{9}$$

where $0 < \lambda \leq 1$ is the EWMA parameter and ζ is a scaling constant. The Shewhart individual chart is indirectly considered for comparison because it is a special case of the EWMA chart when $\lambda = 1$. The EWMA, OGLF, OSLF charts are optimally designed to minimize the zero-state out-of-control ARL while constraining the zero-state in-control ARL to be 500. The out-of-control ARL minimization is for an assumed mean shift shape and magnitude and a shift time-of-occurrence that coincides with the initial observation. Chin and Apley (2006) and Apley and Chin (2007) plot the impulse response coefficients for all of the examples that we consider here. For the EWMA chart, the value of λ is chosen using the same constrained optimization criterion. The thresholds of the CUSCORE and GLRT charts are determined to provide the desired in-control ARL using Monte Carlo simulations and for the design parameters of two, the values that Luceño(1999) and Apley and Shi (1999) recommended are respectively taken. The handicap for the CUSCORE chart was chosen proportional to the feared signal (e.g., $\tilde{\mu}_t/2$) as shown in Equation (5). For the GLRT chart, we used the same window length N (= 20) as recommended in Apley and Shi (1999). Luceño (1999) proposed the two versions of the CUSCORE chart, depending on whether or not the $\tilde{\mu}_t$ in Equation (5) is reinitialized whenever the statistic reaches its zero limit. The CUSCORE without reinitialization is excluded from comparison because of its significant ineffectiveness in the steady state (Runger and Testik 2003; Chin and Apley 2006; Apley and Chin 2007).

3.2 Performance Comparison based on the zero-state ARL

The EWMA and OSLF charts are special cases of the OGLF and thus, cannot perform better than the OGLF. However, the EWMA is included to represent control charts which do not take advantage of the information on the residual mean dynamics and show the performance difference from control charts developed for a time-varying mean shift. As expected, the OGLF, CUSCORE, and GLRT charts outperform the EWMA chart by a wide margin, except for the i.i.d. processes with a step mean shift and other processes with a mean shift of size 0.5 which do not have prominent residual mean dynamics.

For the 32 examples under analysis, <Table 1> shows the zero-state ARLs denoted by ARL_{0zs} and ARL_{1zs}, respectively. The standard errors are in parentheses. The minimum out-of-control ARL for each example is indicated by bold font in each row of <Table 1>. In general, the OGLF or CUSOCRE chart performs best for examples listed in <Table 1>. The superiority of one over the other chart is determined depending on whether the initial dynamics plays a larger role than the lasting effects of the residual mean. The OGLF performs better than the CUSCORE in Examples 5, 6, 20, 21, and 22 where the residual mean has prominent dynamics and rapidly converges to zero or a very small steady state shift and the control charts are expected to rely primarily on the initial dynamics. The opposite is true for Examples 7, 8, 17, 18, 19, 23 and 24 where the residual mean converges to zero very slowly or has a small but considerable steady state shift compared to the significance of initial dynamics. The OGLF chart performs slightly better than the CUSCORE and GLRT for Examples 29~32 with ramp mean shifts, but nearly identically to the OSLF charts and the opti-

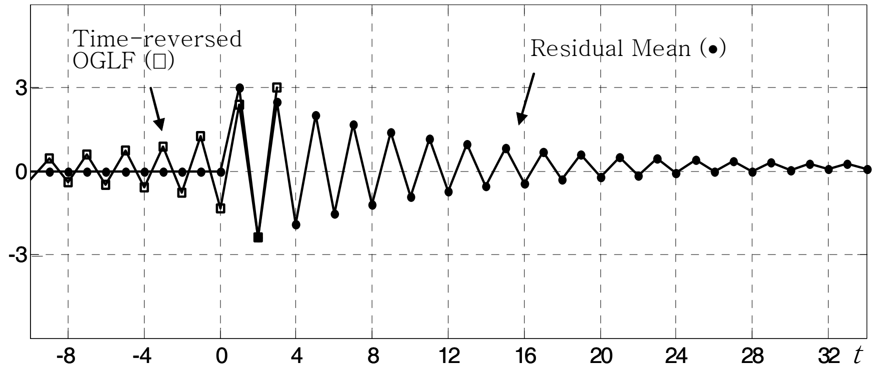

Figure 4. The OGLF for Example 20 applied to the Residual Mean Three Timesteps after the Occurrence of the Shift

mized EWMAs. For the others, they perform comparably. As a simplified version of the OGLF, the OSLF combines the design and implementation efficiency with performance that is substantially better than an optimized EWMA and as good as the OGLF in a number of examples.

Note that the CUSOCRE charts cannot be set up for Examples 9~12 and 25~28. Chin (2008) showed that the CUSCORE chart statistic of Luceño (1999) might totally lose the detection capability. It was illustrated with Examples 9~12 and 25~28. Examples 9~12 have spike mean shifts which have only two non-zero coefficients at the first two timesteps and the remaining zero coefficients as shown in <Figure 3(c)>. Once the CUSUCORE statistic is less than the threshold at $t = 3$, it would continue taking the same value afterward because the term in the bracket of Equation (5) becomes zero and will not have a chance to signal.

For the i.i.d. processes with a step mean shifts (Examples 1~4), CUSUM charts are optimal (Moustakides 1986). As a result, the impulse response of OGLF and OSLF charts are tuned to be virtually identical to those of the optimized EWMA, because an EWMA chart can be designed to approximately perform comparable to any (two-sided) CUSUM chart. The good performance of the CUSCORE chart can also be explained in that the CUSUM and CUSCORE charts coincide for step mean shifts in i.i.d. data.

The OGLF and OSLF charts have many interesting characteristics that result in performance superior to optimized EWMA charts (Chin and Apley 2006; Apley and Chin 2007). According to the ARMA process model and the nature of mean shift, the OGLF and OSLF charts may be tuned to be highly correlated with the residual means, mimic a combined Shewhart-EWMA scheme, or have impulse response coefficients which are reminiscent of the matched filter of the corresponding GLRT chart, as illustrated in the following. For processes with pronounced dynamic patterns of residual mean shifts as in Examples 9~16 and 18~20, the matched filters of the OGLF, OSLF, CUSCORE, and GLRT charts are used to increase the detection probabilities by fostering the correlation with the residual means. The chart statistics in Equations (5), (6), (7), and (8) include the summation of the product of the residuals and the matched filter coefficients. The summation can be viewed as a measure of the correlation between the residuals and the matched filter. Hence, the higher the correlation between two signals, the larger the magnitude of chart statistic. <Figure 4> illustrates how the impulse response coefficients of the OGLF chart statistic for Example 20 forms the correlation with the residual means. The time-reversed coefficients are superimposed on the residual means because the initial coefficients are applied to the most recent observations. As time goes on, the OGLF has high positive correlation and negative correlation by turns, resulting in a large magnitude of the OGLF statistic and a high probability of exceeding its control limits. An analogous mechanism applies to the OSLF, CUSCORE, and GLRT charts. Due to this characteristic, the OGLF ($ARL_{1zs} = 3.1$) for Example 20 dramatically outperforms the optimized EWMA ($ARL_{1zs} = 74.7$).

The OGLF and OSLF charts for Examples 7 and 8 are essentially a weighted combination of a Shewhart chart and an EWMA chart as shown in <Figure 5(a)>. The first two impulse response coefficients correspond to a Shewhart chart filter and the remaining coefficients correspond to an EWMA chart filter. The OGLF and OSLF charts would be expected to behave similar to a combined Shewhart-EWMA scheme (Lucas and Saccucci 1990; Lin and Adams 1996; Lu and Reynolds

1999b; Reynolds and Stoumbos 2001), the only difference being that the latter simultaneously runs two separate chart statistics, while the former combines them into one statistic. Combined Shewhart-EWMA schemes are widely known to work well for processes where the residual mean has a pronounced initial spike and then converges to a small steady-state value. The Shewhart component of combined Shewhart-EWMA schemes is effective at detecting the initial spike and its EWMA component is effective at detecting the lasting small steady state shift, which makes them outperform optimized EWMA charts. <Figure 5(b)> shows the impulse response coefficients of the OGLF and OSLF charts for Examples 25~28, the time-reversed version of which is almost equivalent to those of the residual mean shown in <Figure 3(g)>. The time-reversed OGLF $\{h_j\}$is almost perfectly correlated with the residual mean five timesteps after the shift occurs, and the OGLF performs substantially better than the optimized EWMA for large shifts ($\mu = 3$ and $\mu = 4$).

The GLRT performs slightly better than the OGLF and CUSCORE charts for autocorrelated processes such as Examples 16, 20, and 24 where the mean shift has a considerable lasting effect on the residuals. Runger and Testik (2003) also showed that the GLRT has a better performance over the CUSOCRE chart with reinitialization for similar situations such as an unbounded linear trend mean shift and a sinusoidal mean shift.

4. Robustness Analysis

ARMA model-based approaches have been very popular in SPC applications, but have also suffered the criticism of lacking robustness to inevitable errors in fitting an ARMA model to process data. Since the control charts are designed based on the assumption of no modeling errors, any modeling error affects the control chart performance represented by the in-control ARL, the out-of-control ARL, the false alarm rate, and so forth. Hence, the robustness to modeling errors is a very critical element of control charts required to ensure they perform well in practice.

Most of the research on robustness to modeling errors have focused on empirically studying the effects of modeling errors (e.g. Adams and Tseng 1998; Apley and Shi 1999; Lu and Reynolds 1999a for residual- based charts), but have not investigated it analytically. Exceptions are Apley (2002), Apley and Lee (2003), and Apley and Lee (2008), in which analytical measures were derived for the sensitivity of the in-control performance of control charts with respect to modeling errors, which enables one to quantify and corroborate the empirical findings. The analytical expressions of Apley and Lee (2008) apply to any control chart that can be viewed as the output of a linear filter applied to process data. In this section, we show that the robustness findings from the Monte Carlo simulations for the OGLF, OSLF, EWMA, and Shewhart, and GLRT charts can be explained by the theoretical results of Apley and Lee (2008).

Suppose that the true parameter ϕ_1 differs from the estimate $\hat{\phi}_1$. The residuals generated by Equation (1) are not independent, but actually follows the ARMA (1,1) model

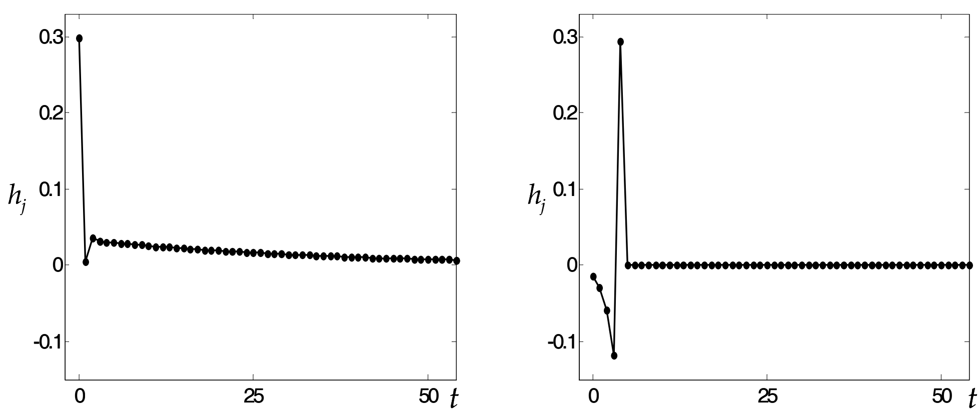

Figure 5. Impulse response coefficients of the OGLF charts : (a) Example 8 and (b) Example 28

$$e_t = \frac{(1-\hat{\phi}_1 B)}{(1-\hat{\theta}_1 B)} x_t = \frac{(1-\hat{\phi}_1 B)}{(1-\hat{\theta}_1 B)} \left[\frac{(1-\theta_1 B)}{(1-\phi_1 B)} a_t + \mu_t \right] = \frac{(1-\hat{\phi}_1 B)}{(1-\phi_1 B)} a_t + \widetilde{\mu}_t, \tag{10}$$

where the "^" symbol denotes an estimate of a quantity. With ϕ_1 underestimated, the residual autocorrelation would be positive and the resulting standard deviation of e_t would be substantially larger than that under the assumption of no modeling error. The increased variance inflates the false alarm rate, which leads to the decrease in the in-control ARL. That is, the effect of modeling errors on the ARL corresponds closely to the effect of modeling errors on the variance of the control chart statistic. Apley and Lee (2008) defined the sensitivity as the partial derivative of the variance of the control chart statistic (which we generically denote by y_t) with respect to the ARMA parameters, scaled by the nominal variance:

$$S(\phi_i) = \frac{\left.\frac{\partial \sigma_y^2}{\partial \phi_i}\right|_{\omega=\hat{\omega}}}{\hat{\sigma}_y^2} \quad : i = 1, 2, \cdots, p, \text{ and} \tag{11}$$

$$S(\theta_i) = \frac{\left.\frac{\partial \sigma_y^2}{\partial \theta_i}\right|_{\omega=\hat{\omega}}}{\hat{\sigma}_y^2} \quad : i = 1, 2, \cdots, q, \tag{12}$$

where $\omega = [\phi_1\ \phi_2 \cdots\ \phi_p\ \theta_1\ \theta_2 \cdots\ \theta_q]^T$ is the vector of ARMA parameters and $\hat{\sigma}_y^2$ is the variance of the control chart statistic when $\omega = \hat{\omega}$. When multiplied by a parameter error (denoted by $\triangle\phi_i$ or $\triangle\theta_i$), Equations (11) and (12) represent the percentage change in the variance, due to modeling errors. Hence, the sensitivity measures can be viewed as the analytical percentage variance changes (PVC) for modeling errors, which are compared with the empirical PVCs in <Table 3>. The analytical PVCs agree reasonably well with the empirical PVCs and are also fairly consistent with the percentage ARL changes, in the sense that larger PVC values almost always correspond to larger ARL percentage changes. Although it would be more desirable to directly consider the sensitivity of the ARL, it is unfortunately too analytically intractable. As shown in Equations (11) and (12), instead, the standardized variance changes with respect to modeling errors are proposed as the indirect measures for their corresponding ARL changes of control charts.

Using Equations (11) and (12), we derive the following sensitivity measures for the GLRT, OGLF, and OSLF charts applied to e_t. See Appendix I for the detailed derivation. These measures reduce to relatively simple expressions for the ARMA(1, 1) processes considered in Section 3. For each $T_\xi(t)$ of the GLRT applied to the residuals defined in Equation (1),

$$S_{e,GLRT}(\phi_1, \xi) = 2\sum_{k=0}^{\infty} P_k \rho_{1+k} = 2\sum_{k=0}^{\xi-2} \phi_1^k \left(\frac{\sum_{j=1}^{\xi-k-1} \widetilde{\mu}_j \widetilde{\mu}_{j+k+1}}{\sum_{j=1}^{\xi} \widetilde{\mu}^2} \right)$$

$$S_{e,GLRT}(\theta_1, \xi) = 2\sum_{k=0}^{\infty} Q_k \rho_{1+k} = -2\sum_{k=0}^{\xi-2} \theta_1^k \left(\frac{\sum_{j=1}^{\xi-k-1} \widetilde{\mu}_j \widetilde{\mu}_{j+k+1}}{\sum_{j=1}^{\xi} \widetilde{\mu}^2} \right).$$

For the OGLF defined in Equation (7),

$$S_{e,OGLF}(\phi_1) = \frac{2}{\sum_{j=0}^{Tr} h_j^2} \sum_{k=0}^{Tr-2} \phi_1^k \left(\sum_{j=0}^{Tr-k-1} h_j h_{j+k+1} \right)$$

$$S_{e,OGLF}(\theta_1) = -\frac{2}{\sum_{j=0}^{Tr} h_j^2} \sum_{k=0}^{Tr-2} \theta_1^k \left(\sum_{j=0}^{Tr-k-1} h_j h_{j+k+1} \right).$$

For the OSLF defined in Equation (8),

$$S_{e,OSLF}(\phi_1) = \frac{2}{1-\alpha_1\phi_1-\alpha_2\phi_1^2} \left(\alpha_2\phi_1 + \frac{a_1\lambda_1 + a_2\lambda_2}{a_1 + a_2} \right)$$

$$S_{e,OSLF}(\theta_1) = -\frac{2}{1-\alpha_1\theta_1-\alpha_2\theta_1^2} \left(\alpha_2\theta_1 + \frac{a_1\lambda_1 + a_2\lambda_2}{a_1 + a_2} \right)$$

where

$$a_1 = -\frac{(\lambda_1-\beta)(1-\beta\lambda_1)}{(1-\lambda_1^2)},$$

$$a_2 = \frac{(\lambda_2-\beta)(1-\beta\lambda_2)}{(1-\lambda_2^2)},$$

$$\lambda_1, \lambda_2 = \frac{1}{2}\left(\alpha_1 \pm \sqrt{\alpha_1^2 + 4\alpha_2} \right).$$

For the EWMA chart defined in Equation (9), as a special case of the OSLF chart when $\alpha_1 = (1-\lambda)$, $\alpha_2 = \beta = 0$, and $\gamma = \zeta$,

Table 2. Sensitivities for the OGLF, the OSLF, the optimal EWMA, and the GLRT when the one of the true parameters of an ARMA(1,1) process is incorrectly estimated (ϕ_1 = 0.89 vs. $\hat{\phi}_1$ = 0.9 and θ_1 = -0.89 vs. $\hat{\theta}_1$ = -0.9)

No.	Time Series Model ϕ_1	θ_1	Shift Type	Size	OGLF $S_e(\phi_1)$	$S_e(\theta_1)$	OSLF $S_e(\phi_1)$	$S_e(\theta_1)$	Optimal EWMA $S_e(\phi_1)$	$S_e(\theta_1)$	GLRT $S_e(\phi_1)$	$S_e(\theta_1)$
1	0	0	Step	0.5	1.906	-1.906	1.906	-1.906	1.906	-1.906	**1.800**	**-1.800**
2	0	0	Step	1.5	**1.516**	**-1.516**	**1.516**	**-1.516**	**1.516**	**-1.516**	1.800	-1.800
3	0	0	Step	3	**0.648**	**-0.648**	**0.648**	**-0.648**	**0.648**	**-0.648**	1.800	-1.800
4	0	0	Step	4	**0.226**	**-0.226**	**0.226**	**-0.226**	**0.226**	**-0.226**	1.800	-1.800
5	0.9	0	Step	0.5	19.607	-1.996	19.607	-1.996	19.607	-1.996	**1.651**	**-0.330**
6	0.9	0	Step	1.5	18.683	-1.986	18.683	-1.986	18.683	-1.986	**1.651**	**-0.330**
7	0.9	0	Step	3	6.914	-0.782	6.717	-0.742	16.468	-1.958	**1.651**	**-0.330**
8	0.9	0	Step	4	3.958	-0.360	3.960	-0.360	14.337	-1.924	**1.651**	**-0.330**
9	0.9	0	Spike	0.5	-1.014	1.197	-0.999	1.107	**0**	**0**	-0.994	0.994
10	0.9	0	Spike	1.5	-1.006	1.069	-0.999	1.099	**0**	**0**	-0.994	0.994
11	0.9	0	Spike	3	-1.003	1.044	-0.999	1.093	**0**	**0**	-0.994	0.994
12	0.9	0	Spike	4	-1.001	1.033	-0.999	1.096	**0**	**0**	-0.994	0.994
13	0	0	Sinusoid	S_1	-1.815	1.815	-1.815	1.815	**0**	**0**	-1.800	1.800
14	0	0	Sinusoid	S_2	0.018	-0.018	0.018	-0.018	**0**	**0**	**0**	**0**
15	0	0	Sinusoid	S_3	1.430	-1.430	1.443	-1.443	**0.784**	**-0.784**	1.286	-1.286
16	0	0	Sinusoid	S_4	1.217	-1.217	1.387	-1.387	**0.768**	**-0.768**	1.286	-1.286
17	0.9	-0.9	Step	0.5	19.607	**-1.052**	19.607	**-1.052**	19.607	**-1.052**	**-0.887**	6.298
18	0.9	-0.9	Step	1.5	1.683	11.641	-1.006	11.408	19.416	**-1.051**	**-0.887**	6.298
19	0.9	-0.9	Step	2	-1.006	11.410	-1.006	11.408	19.228	**-1.050**	**-0.887**	6.298
20	0.9	-0.9	Step	3	-0.720	6.715	-0.922	5.745	**0**	**0**	**-0.887**	6.298
21	0.9	0.5	Step	0.5	19.200	-3.967	19.228	-3.969	19.228	-3.969	**4.506**	**-2.171**
22	0.9	0.5	Step	1.5	16.468	-3.836	16.468	-3.836	16.468	-3.836	**4.506**	**-2.171**
23	0.9	0.5	Step	3	8.460	-3.143	8.469	-3.154	8.462	-3.143	**4.506**	**-2.171**
24	0.9	0.5	Step	4	**3.921**	**-1.609**	3.726	-2.135	3.726	-2.135	4.506	-2.171
25	0.9	0.5	Spike	0.5	-0.876	0.654	-0.334	0.361	**0**	**0**	-0.879	0.645
26	0.9	0.5	Spike	1.5	-0.876	0.654	-0.105	0.110	**0**	**0**	-0.879	0.645
27	0.9	0.5	Spike	3	-0.876	0.654	-0.068	0.069	**0**	**0**	-0.879	0.645
28	0.9	0.5	Spike	4	-0.876	0.654	-0.129	0.137	**0**	**0**	-0.879	0.645
29	0	0	Ramp	0.5	1.954	-1.954	1.954	-1.954	1.992	-1.992	**1.714**	**-1.714**
30	0	0	Ramp	1.5	1.790	-1.790	1.790	-1.790	1.954	-1.954	**1.714**	**-1.714**
31	0	0	Ramp	3	**1.511**	**-1.511**	**1.511**	**-1.511**	1.838	-1.838	1.714	-1.714
32	0	0	Ramp	4	**1.345**	**-1.345**	**1.345**	**-1.345**	1.734	-1.734	1.714	-1.714

$$S_{e,EWMA}(\phi_1) = \frac{2(1-\lambda)}{1-\phi_1(1-\lambda)}$$

$$S_{e,EWMA}(\theta_1) = -\frac{2(1-\lambda)}{1-\theta_1(1-\lambda)}.$$

For the Shewhart chart as a special case of the EWMA chart when $\lambda = 1$,

$$S_{e,Shewhart}(\phi_1) = S_{e,Shewhart}(\theta_1) = 0.$$

<Table 2> shows the sensitivities for the 32 Examples considered in Section 3. The minimum sensitivity for each example is indicated by bold font. Several interesting characteristics are revealed. As shown in Equations (A.1) and (A.2), the sensitivities are the

weighted sum of the impulse response coefficients of the AR and MA polynomials of the original process, where the weights are given by the autocorrelation function of the control chart statistic. Specifically, the sensitivities mainly rely on the type (positive or negative) and decay rate of autocorrelation functions of the control chart statistic and AR and MA polynomials of the original process. The more slowly decaying the autocorrelation functions, typically the higher the sensitivities. Hence, the sensitivity of a control chart may change for different original processes. The EWMA charts for 11 of 32 examples reduce to a Shewhart chart, which has zero sensitivities. Consider the EWMA charts for the remaining 21 examples, for which the chart statistics have positive autocorrelation. The magnitudes of their sensitivities can be explained in the light of the autocorrelation of the original processes. For Examples 1~4, 15~16, and 29~32 in which the original processes are i.i.d., the sensitivities for both ϕ and θ are low. For Examples 5~8, 17~19, and 21~24, the AR polynomials have highly positive autocorrelation and thus, the sensitivities for ϕ are high. On the other hand, the sensitivities for θ are relatively low due to the MA polynomials of Examples 5~8 with no autocorrelation, those of Examples 17~19 with negative autocorrelation, and those of Examples 21~24 with low positive autocorrelation.

For i.i.d. processes ($\theta = \phi = 0$), both sensitivities are the same because the autocorrelations of the $\Phi^{-1}(B)$ and $\Theta(B)$ are identical. Except for processes such as Examples 2~4, 9~20, 25~28, 31, and 32 in which the optimally tuned EWMA charts turn out to have large λ's resulting in very small moving window lengths (e.g., it becomes a Shewhart chart with $\lambda = 1$ for Examples 9~14 and 25~28) or when the MA polynomial of the original process has negative autocorrelation, the GLRT chart has the lowest sensitivities (i.e., the most robust) to the modeling error due to the small number of impulse response coefficients constituting a moving window, and the OGLF are at least as robust as the EWMA is. Note that the GLRT chart consistently has small sensitivities for all examples, but the EWMA chart does not such as for Examples 5~8, 17~19, and 21~22. While the moving window length of the GLRT chart is fixed (i.e., $N = 20$), those of the OGLF, OSLF, and EWMA chart are optimally determined according to the magnitude of the feared signal through the design procedures. For the same type of feared signal, the sensitivities tend to get smaller as the magnitude of the feared signal increases. In order to increase the detection probability in this case, a control chart is designed to place more weight on recent observations to improve the detection of mean shifts of large magnitude, which leads to a control chart with fast-decaying autocorrelation function. For instance, the λ's of the EWMA charts for Examples 1~4 are 0.047, 0.242, 0.676, and 0.887, respectively. Since the impulse response coefficients $\{g_j\}$ of the EWMA are $(1-\lambda)^j$, the EWMA chart has the largest λ for the largest feared signal and has the smallest sensitivities. This is consistent with the sensitivity expressions in Equations (A.1) and (A.2). This fact implies that EWMA charts with other larger non-optimal λ's would be more robust, even though their performance are a little bit worsened. Apley and Lee (2003) also found that larger values of λ do indeed result in better robustness. However, the performance for small shifts may be so much worse for larger values of λ that a more attractive alternative is to use a smaller value of λ but use control limits that are wider than normal to prevent an excessive number of false alarms. Apley and Lee (2003) and Apley (2002) also presented methods for suitably widening the control limits for this purpose.

The $S_{e,GLRT}(\phi_1,\xi)$ and $S_{e,GLRT}(\theta_1,\xi)$ of the GLRT are identical for the same type of mean shift regardless of magnitude, respectively, because the same unit magnitude feared signal is used as a matched filter. Note that the sinusoidal means for Examples 13 and 14 have different periods, which results in different sensitivities, whereas the sensitivities are the same for Example 15 and 16 of the same period. We calculate the sensitivities of the GLRT for only one of the GLRT statistics (e.g., for a mean shift occurring at only one of the N timesteps within the window). We chose $\xi = 10$ in the following examples, because it is in the mid range of all the ζ values in Equation (6) and most reasonably represents the sensitivity of the GLRT.

We consider two situations that ϕ_1 and θ_1 are incorrectly estimated for Examples 17~20 (let the parameter values listed in <Table 1> represent the estimated parameters). Suppose that the values of true parameters are $\phi_1 = 0.89$ and $\theta_1 = -0.9$ in one situation and $\phi_1 = 0.9$ and $\theta_1 = -0.89$ in the second situation. For these errors in estimating ϕ_1 and θ_1, respectively, Equation (10) implies that the residuals with no mean shift obey the models

$$e_t = \frac{(1-0.9B)}{(1-0.89B)} a_t \text{ and } e_t = \frac{(1+0.89B)}{(1+0.9B)} a_t,$$

respectively. The Monte Carlo simulations with 100,000 replicates are used to compare the analytical results of sensitivities with empirical results. The actual PVC, the first-order approximation of the PVC based on sensitivity measures, and corresponding in-control ARLs for the incorrectly estimated parameters are shown in <Table 3>. The actual PVCs agree reasonably well with the approximations, and the close correspondence between the PVCs and the percentage

Table 3. Comparison of the Analytical Results of Sensitivities with Empirical Results for Examples 17~20

No.	*Estimated parameter* $\hat{\phi}_1$	$\hat{\theta}_1$	*Shift* Type	Size	*True parameter* ϕ_1	θ_1	*OGLF* $PVC(\phi_1)$ / $S_e(\phi_1)\Delta\phi_1$; $PVC(\theta_1)$ / $S_e(\theta_1)\Delta\theta_1$	ARL_{0,ϕ_1} (std. err.); ARL_{0,θ_1} (std. err.)	*OSLF* $PVC(\phi_1)$ / $S_e(\phi_1)\Delta\phi_1$; $PVC(\theta_1)$ / $S_e(\theta_1)\Delta\theta_1$	ARL_{0,ϕ_1} (std. err.); ARL_{0,θ_1} (std. err.)	*Optimized EWMA* $PVC(\phi_1)$ / $S_e(\phi_1)\Delta\phi_1$; $PVC(\theta_1)$ / $S_e(\theta_1)\Delta\theta_1$	ARL_{0,ϕ_1} (std. err.); ARL_{0,θ_1} (std. err.)	*GLRT* $PVC(\phi_1)$ / $S_e(\phi_1)\Delta\phi_1$; $PVC(\theta_1)$ / $S_e(\theta_1)\Delta\theta_1$	ARL_{0,ϕ_1} (std. err.); ARL_{0,θ_1} (std. err.)
17	.9	-.9	Step	.5	.89	-.9	-17.043	611.73	-17.036	611.48	-17.036	611.89	0.902	482.03
							-19.607	(1.67)	-19.607	(1.67)	-19.607	(1.67)	0.887	(1.51)
					.9	-.89	-1.050	511.06	-1.050	510.78	-1.050	510.34	6.487	434.67
							-1.052	(1.39)	-1.052	(1.39)	-1.052	(1.38)	6.298	(1.37)
					.87	-.9	-40.198	901.34	-40.201	898.77	-40.201	906.22	2.793	448.08
							-58.821	(2.50)	-58.821	(2.50)	-58.821	(2.52)	2.661	(1.40)
					.9	-.87	-3.135	522.56	-3.122	521.35	-3.122	522.20	20.555	323.31
							-3.156	(1.42)	-3.156	(1.41)	-3.156	(1.42)	18.894	(1.01)
18	.9	-.9	Step	1.5	.89	-.9	-1.452	531.18	1.033	484.28	-16.895	621.38	0.902	480.71
							-1.683	(1.58)	1.006	(1.49)	-19.416	(1.72)	0.887	(1.50)
					.9	-.89	12.211	382.26	12.103	373.76	-1.062	509.25	6.487	436.40
							11.641	(1.10)	11.408	(1.15)	-1.051	(1.40)	6.298	(1.38)
					.87	-.9	-2.904	570.44	3.173	453.30	-39.892	953.12	2.793	455.10
							-5.049	(1.69)	3.018	(1.40)	-58.248	(2.69)	2.661	(1.43)
					.9	-.87	40.330	248.08	39.705	230.39	-3.128	522.19	20.555	323.86
							34.923	(0.68)	34.224	(0.69)	-3.153	(1.44)	18.894	(1.01)
19	.9	-.9	Step	2	.89	-.9	1.036	476.16	1.033	483.16	-16.737	629.58	0.902	480.58
							1.006	(1.47)	1.006	(1..49)	-19.228	(1.77)	0.887	(1.51)
					.9	-.89	11.991	368.10	12.103	371.35	-1.053	510.63	6.487	433.45
							11.410	(1.12)	11.408	(1.14)	-1.050	(1.42)	6.298	(1.36)
					.87	-.9	3.109	446.96	3.173	451.21	-39.607	1011.6	2.793	450.01
							3.018	(1.38)	3.018	(1.39)	-57.684	(2.93)	2.661	(1.42)
					.9	-.87	39.600	228.89	39.705	230.94	-3.137	527.98	20.555	323.57
							34.230	(0.69)	34.224	(0.70)	-3.150	(1.48)	18.894	(1.00)
20	.9	-.9	Step	3	.89	-.9	0.783	487.67	0.965	480.10	0.096	501.69	0.902	479.44
							0.720	(1.53)	0.922	(1.50)	0.000	(1.59)	0.887	(1.50)
					.9	-.89	7.137	396.28	6.140	402.12	0.096	499.33	6.487	434.46
							6.715	(1.24)	5.745	(1.26)	0.000	(1.57)	6.298	(1.35)
					.87	-.9	2.437	460.42	2.895	445.65	0.382	493.23	2.793	446.10
							2.160	(1.43)	2.766	(1.40)	0.000	(1.56)	2.661	(1.40)
					.9	-.87	23.499	261.02	20.263	272.64	0.478	488.59	20.555	321.63
							20.145	(0.80)	17.235	(0.85)	0.000	(1.53)	18.894	(1.00)

changes in ARLs implies that the sensitivity measures are appropriate as the indirect measures for the ARL change of control charts with respect to modeling errors.

For Example 18, the OSLF and EWMA chart statistics are recursively calculated by $y_t = 0.1399(1+0.039B)(1+0.924B-0.007B)^{-1}e_t$ and $y_t = 0.557(1-0.997B)^{-1}e_t$, respectively (Chin and Apley 2006). The respective variances for both charts under the assumption of no modeling error are 0.1355 and 0.5179. To illustrate the effects of modeling errors, we calculate the variances for both charts experiencing the preceding modeling error in which only one of the two parameters is incorrectly estimated. With ϕ_1 overestimated, the actual variance for the OSLF chart is 0.1369 which is 1.03% larger than the assumed one. This PVC 1.03% is consistent with the analytical result that the approximate percentage variance increase in the OSLF variance is $S_{e,OSLF}(\phi_1)(\phi_1 - \hat{\phi}_1)$ = 1.01%. The actual PVC leads to the decrease in the in-control ARL from 500 to 484. With θ_1 underestimated, the actual variance for the OSLF chart is 0.1519 which is 12.10% larger than the assumed one. This PVC 12.10% is also consistent with the analytical result that the approximate percentage variance increase is 11.41%, decreasing the in-control ARL from 500 to 374. For ϕ_1 and θ_1 of the EWMA chart, the analytical percentage variance decreases are 19.42% and 1.06%, which agree reasonably well with the actual percentage variance decreases 16.90% and 1.05%, respectively. These increases (decreases) in the variance of the chart statistic result in higher (lower) false alarm rates, which decrease (increase) the in-control ARL. The in-control ARLs for the OSLF chart decrease by 3.14% and 25.25% for the true ϕ_1 and θ_1. Those for the EWMA chart increase by 24.27% and 1.85%, respectively. The difference between the changes of the variance and performance can be explained in that performance change of a control charting scheme is affected by its autocorrelation level as well as its variance with the control limits fixed (Jiang and Tsui 2001). However, the sensitivities provide fairly reasonable comparison for the robustness to modeling error. In addition, the sign of the sensitivity indicates whether the variance and ARL will increase or decrease for a particular type of modeling error. The negative sign of the $S_{e,OSLF}(\phi_1)$ for Example 18 imply that the underestimation of ϕ_1 results in an increase in variance and a decrease in ARL.

While the ±0.01 parameter errors may seem small, they may actually have a substantial effect on the performance. For example, the first row of <Table 3> shows that an error of 0.01 in the AR parameter causes a 17% decrease in the variance of the EWMA and OGLF statistics, which is substantial. The surprisingly large sensitivity of the charts underscores the need for analytical sensitivity expressions that explain the mechanisms behind the lack of robustness of certain charts. Because larger parameter errors are also of interest, we extend this analysis to the parameter errors of ±0.03, and the results are shown in <Table 3>. The difference among the analytical results of sensitivities and the changes of the variances and performances becomes larger, because the sensitivity is based on a first-order partial derivative. Note that the sensitivities still provide a reasonable basis for comparison, however. For the OSLF with incorrectly estimated ϕ_1 and θ_1 in Example 18 aforementioned, the PVCs 3.17% and 39.71% are still fairly consistent with the analytical result 3.02% and 34.22%, respectively. The PVC -3.13% for the EWMA chart with θ_1 underestimated is also consistent with the analytical result -3.15%. For the EWMA chart with ϕ_1 overestimated, the difference between the analytical approximation and actual PVC gets to be larger from 14.9% (for the parameter error of +0.01) to 46.0% (for the parameter error of +0.03). Similar augmentations are found in other examples. For all of Examples 17~20 under analysis, however, this inevitable augmentation does not have any influence on selecting the most robust chart and does not blur distinct difference between sensitivities of control charts.

5. Conclusions

In this paper, we have surveyed control charting schemes for autocorrelated data, with a focus on performance and robustness of residual-based control charts. In the ARL comparison using Monte Carlo simulations, the OGLF, OSLF, CUSOCRE, and GLRT charts substantially outperform the optimized EWMA chart which does not take advantage of the information hidden in the dynamic characteristics of the residual mean. For the i.i.d. processes with a step mean shift, for which there are no prominent dynamics in the residuals, the first three control charts perform comparably to the EWMA chart. Generally, the

OGLF or CUSCORE chart performs the best. The OGLF chart perform better for processes in which the residual mean settles down to zero or a very small steady-state value after experiencing initial prominent dynamics. The CUSCORE chart is more effective at detecting a residual mean decaying slowly and converging to a relatively significant steady-state value. One drawback of the CUSCORE chart with re-initialization is that it may totally lose the ability to detect a shift when the feared signal converges to zero after few initial spikes. The GLRT performs worse than the EWMA for processes with a short-lived minor residual mean shift such as Example 5 and 21.

The robustness to modeling errors is a critical characteristic that should be considered when selecting and designing a control chart. To investigate the robustness of the control charts under consideration, we derived analytical expressions for their sensitivity to ARMA modeling errors and demonstrated their validity by comparing the analytical results with the actual PVCs and the ARLs calculated using Monte Carlo simulations. The sensitivity of a chart depends primarily on the autocorrelation of the chart statistic and AR and MA polynomials of the original process. The more slowly decaying the autocorrelation, the higher the sensitivities in general. The GLRT is the most robust among the control charts developed for detecting a pre-specified time-varying mean shift.

No control chart is consistently superior to others in terms of performance and robustness. However, if it is possible to quantify the performance and robustness of a control chart based on the information known a priori about the original process and the nature of the mean shift of interest, it would aid in selecting a control chart more appropriately. The survey and empirical and analytical results in this paper were provided for this purpose.

<Appendix I>

For the output $y_t = H(B)x_t$ of a general linear filter applied to an ARMA(p, q) process x_t, Apley and Lee (2008) derived the following expressions for the sensitivity measures defined in Equations (11) and (12):

$$S(\phi_i) = 2\sum_{k=0}^{\infty} P_k \rho_{i+k}: i = 1, 2, \cdots, p, \text{ and} \tag{A.1}$$

$$S(\theta_i) = -2\sum_{k=0}^{\infty} Q_k \rho_{i+k}: i = 1, 2, \cdots, q, \tag{A.2}$$

where ρ_j denotes the autocorrelation function of y_t under the assumption of no modeling errors at lag j and $\{P_j : j = 0, 1, 2, \cdots\}$ and $\{Q_j : j = 0, 1, 2, \cdots\}$ denote the impulse response coefficients of $\Phi^{-1}(B) = \sum_{j=0}^{\infty} P_j B^j$ and $\Theta^{-1}(B) = \sum_{j=0}^{\infty} Q_j B^j$, respectively. We derive the sensitivities for the GLRT, OGLF, and OSLF charts applied to the residuals of ARMA(1, 1) processes with parameter ϕ_1 and θ_1 under assumption that $a_t \sim NID(0, 1)$.

For the GLRT chart defined in Equation (6) (Apley and Shi 1999), the variance and covariance functions for the Generalized Likelihood Ratio (GLR) statistic with a moving window of length ζ are defined as

$$\gamma_{0,\xi} = E(T_\xi(t)\,T_\xi(t)) = 1 \text{ and}$$
$$\gamma_{k,\xi} = E(T_\xi(t)\,T_\xi(t+k)) = \left(\sum_{j=1}^{\xi}\tilde{\mu}_j^2\right)^{-1} \sum_{j=1}^{\xi-k}\tilde{\mu}_j\tilde{\mu}_{j+k}\,.$$

The autocorrelation function is obtained as

$$\rho_{k,\xi} = \frac{\gamma_{k,\xi}}{\gamma_{0,r}} = \frac{\sum_{j=1}^{\xi-k}\tilde{\mu}_j\tilde{\mu}_{j+k}}{\sum_{j=1}^{\xi}\tilde{\mu}_j^2}.$$

Based on the general expressions of the sensitivity measures (Apley and Lee 2008), the sensitivity measures for ARMA(1,1) processes are approximated by

$$S_{e,GLRT}(\phi_1,\xi) = 2\sum_{k=0}^{\infty} P_k\rho_{1+k} = 2\sum_{k=0}^{\xi-2}\phi_1^k\left(\frac{\sum_{j=1}^{\xi-k-1}\tilde{\mu}_j\tilde{\mu}_{j+k+1}}{\sum_{j=1}^{\xi}\tilde{\mu}_j^2}\right) \text{ and}$$

$$S_{e,GLRT}(\theta_1,\xi) = 2\sum_{k=0}^{\infty} Q_k\rho_{1+k} = -2\sum_{k=0}^{\xi-2}\theta_1^k\left(\frac{\sum_{j=1}^{\xi-k-1}\tilde{\mu}_j\tilde{\mu}_{j+k+1}}{\sum_{j=1}^{\xi}\tilde{\mu}_j^2}\right).$$

The variance, covariance, and autocorrelation functions of the OGLF chart (Apley and Chin 2007) are given by

$$\gamma_0 = Cov(y_t, y_t) = Var(y_t) = \sum_{j=0}^{Tr} h_j^2\,,$$

$$\gamma_k = Cov(y_t, y_{t+k}) = \sum_{j=0}^{Tr-k} h_j h_{j+k} \text{, and } \rho_k = \frac{\gamma_k}{\gamma_0} = \frac{\sum_{j=0}^{Tr-k} h_j h_{j+k}}{\sum_{j=0}^{Tr} h_j^2}.$$

The sensitivity measures for ARMA(1,1) processes are defined as

$$S_{e,OGLF}(\phi_1) = \frac{2}{\sum_{j=0}^{Tr} h_j^2} \sum_{k=0}^{Tr-2} \phi_1^k \left(\sum_{j=0}^{Tr-k-1} h_j h_{j+k+1} \right) \text{ and}$$

$$S_{e,OGLF}(\theta_1) = -\frac{2}{\sum_{j=0}^{Tr} h_j^2} \sum_{k=0}^{Tr-2} \theta_1^k \left(\sum_{j=0}^{Tr-k-1} h_j h_{j+k+1} \right).$$

For the OSLF chart defined as Equation (8), the autocorrelation function is defined as (Pandit and Wu 1983)

$$\rho_k = \frac{1}{a_1 + a_2} \left(a_1 \lambda_1^k + a_2 \lambda_2^k \right)$$

where,

$$a_1 = -\frac{(\lambda_1 - \beta)(1 - \beta\lambda_1)}{(1 - \lambda_1^2)}, \quad a_2 = \frac{(\lambda_2 - \beta)(1 - \beta\lambda_2)}{(1 - \lambda_2^2)}, \text{ and}$$

$$\lambda_1, \lambda_2 = \frac{1}{2}\left(\alpha_1 \pm \sqrt{\alpha_1^2 + 4\alpha_2} \right).$$

The sensitivity measures for ARMA(1,1) processes are calculated by

$$S_{e,OSLF}(\phi_1) = \frac{2}{1 - \alpha_1\phi - \alpha_2\phi^2} \left(\alpha_2\phi + \frac{a_1\lambda_1 + a_2\lambda_2}{a_1 + a_2} \right) \text{ and}$$

$$S_{e,OSLF}(\theta_1) = -\frac{2}{1 - \alpha_1\theta - \alpha_2\theta^2} \left(\alpha_2\theta + \frac{a_1\lambda_1 + a_2\lambda_2}{a_1 + a_2} \right).$$

References

Adams, B. M. and Tseng, I. T. (1998), Robustness of Forecast-Based Monitoring Schemes, *Journal of Quality Technology*, **30**(4), 328-339.

Alwan, L. C. (1992), Effects of Autocorrelation on Control Chart Performance, *Communications in Statistics: Theory and Method*, **21**(4), 1025-1049.

Alwan, L. C. and Roberts, H. V. (1988), Time-Series Modeling for Statistical Process Control, *Journal of Business & Economic Statistics*, **6**(1), 87-95.

Apley, D. W. (2002), Time Series Control Charts in the Presence of Model Uncertainty, *ASME Journal of Manufacturing Science and Engineering*, **124**(4), 891-898.

Apley, D. W. and Chin, C. (2007), An Optimal Filter Design Approach to Statistical Process Control, *Journal of Quality Technology*, **39**(2), 93-117.

Apley, D. W. and Lee, H. C. (2003), Design of Exponentially Weighted Moving Average Control Charts for Autocorrelated Processes with Model Uncertainty, *Technometrics*, **45**(3), 187-198.

Apley, D. W. and Lee, H. C. (2008), Robustness Comparison of Exponentially Weighted Moving Average Charts on Autocorrelated Data and on Residuals, *Journal of Quality Technology,* to appear.

Apley, D. W. and Shi, J. (1999), GLRT for Statistical Process Control of Autocorrelated Processes, *IIE Transactions*, **31**(12), 1123-1134.

Bagshaw, M. and Johnson, R. A. (1975), The Effect of Serial Correlation on the Performance of CUSUM Tests II, *Technometrics*, 17(1), 73-80.

Bagshaw, M. and Johnson R. A. (1977), Sequential Procedures for Detecting Parameter Changes in a Time-Series Model, *Journal of the American Statistical Association*, **72**(359), 593-597.

Berthouex, P. M., Hunter, E. and Pallesen, L. (1978), Monitoring Sewage Treatment Plants: Some Quality Control Aspects, *Journal of Quality Technology,* **10**(4), 139-149

Box, G. E. P., Jenkins, G., and Reinsel, G. (1994), *Time Series Analysis, Forecasting, and Control, 3rd ed.*, Prentice-Hall, Englewood Cliffs, NJ.

Box, G. E. P. and Ramírez, J. (1992), Cumulative Score Charts, *Quality and Reliability Engineering International*, **8**(1), 1727.

Box, G. E. P. and Luceño, A. (1997), *Statistical Control by Monitoring and Feedback Adjustment*, Wiley, New York, NY.

Chin, C. (2008), Modified Cuscore Charts for Autocorrelated Processes, *to be submitted*.

Chin, C. and Apley, D. W. (2006), Optimal Design of Second-Order Linear Filters for Control Charting. *Technometrics*, **48**(3) 337-348.

English, J. R., Lee, S-c., Martin, T. W., and Tilmon, C. (2000), Detecting Changes in Autoregressive Processes with X-bar and EWMA charts, *IIE Transactions*, **32**(12) 1103-1113.

Fisher, R. A. (1925), Theory of Statistical Estimation, *Proceeding of the Cambridge Philosophical Society*, **22**, 700-725.

Goldsmith, P. L. and Whitefield, H. (1961), Average Run Lengths in Cumulative Chart Quality Control Schemes, *Technometrics*, **3**(1), 11-20.

Harris, T. J. and Ross, W. H. (1991), Statistical Process Control Procedures for Correlated Observations, *Canadian Journal of Chemical Engineering*, **69**, 48-57.

Hunter, J. S. (1986), The Exponentially Weighted Moving Average, *Journal of Quality Technology*, 18(4), 203-210.

Jiang W. and Tsui, K. (2001), Some Properties of the ARMA Control Chart, *Nonlinear Analysis*, 47, 2073-2088.

Jiang, W., Tsui, K. and Woodall, W. H. (2000), A New SPC Monitoring Method: The ARMA Chart, *Technometrics*, **42** (4), 399-410.

Johnson, R. A. and Bagshaw, M. (1974), The Effect of Serial Correlation on the Performance of CUSUM Tests, *Technometrics,* **16**(1), 103-112.

Lin, S. W., and Adams, B. M. (1996), Combined Control Charts for Forecast-Based Monitoring Schemes, *Journal of Quality Technology*, **28**(3), 289-301.

Luceño, A. (1999), Average Run Lengths and Run Length Probability Distributions for Cuscore Charts to Control Normal Mean, *Computational Statistics and Data Analysis,* **32**(2), 177-195.

Lu, C. and Reynolds, M. R., Jr. (1999a), EWMA Control Charts for Monitoring the Mean of Autocorrelated Processes, *Journal of Quality Technology*, **31**(2), 166-188.

Lu, C. and Reynolds, M. R., Jr. (1999b), Control Charts for Monitoring the Mean and Variance of Autocorrelated Processes. *Journal of Quality Technology*, **31**(3), 259-274.

Lucas, J. M. and Saccucci, M. S. (1990), Exponentially Weighted Moving Average Control Schemes: Properties and Enhancements, *Technometrics*, **32**(1), 1-12.

Luceño, A. (2004), Cuscore Charts to Detect Level Shifts in Autocorrelated Noise, *Quality Technology and Quantitative Management*, **1**(1), 27-45.

Montgomery, D. C. (2005), *Introduction to Statistical Quality Control, 5th ed.*, Wiley, New York, NY.

Montgomery, D. C. and Mastrangelo, C. M. (1991), Some Statistical Process Control Methods for Autocorrelated Data*,* *Journal of Quality Technology*, **23**(3), 179-193.

Montgomery, D. C. and Woodall, W. H. (1997), A Discussion of Statistically-Based Process Monitoring and Control, *Journal of Quality Technology*, **29**(2), 121-162.

Moustakides, G. (1986), Optimal Stopping Times for Detecting Changes in Distributions. *Annals of Statistics,* **14**(4), 1379-1387.

Page, E. S. (1955), A Test for a Change in a Parameter Occurring at an Unknown Point, *Biometrica*, **42**(3/4), 523-527.

Pandit, S. M., and Wu, S. M. (1983), *Time Series and System Analysis, With Applications*, New York: John Wiley.

Reynolds, M. R., Jr., and Stoumbos, Z. (2001), Monitoring the Process Mean and Variance Using Individual Observations and Variable Sampling Intervals, *Journal of Quality Technology*, **33**(2), 181-205.

Roberts, S. W. (1959),Control Chart Tests Based on Geometric Moving Averages, *Technometrics*, **1**(3), 239-250.

Runger, G. C. and Testik, M. C. (2003), Control Charts for Monitoring Fault Signatures: Cuscore versus GLR, *Quality and Reliability Engineering International* **19**, 387-396.

Runger, G. C., Willemain, T. R., and Prabhu, S. (1995), Average Run Lengths for CUSUM Control Charts Applied to Residuals, *Communications in Statistics - Theory and Methods*, **24**(1), 273-282.

Shu, L., Apley, D. W., and Tsung, F. (2002), Autocorrelated Process Monitoring Using Triggered Cuscore Charts, *Quality and Reliability Engineering International*, **18**, 411-421.

Stoumbos, Z. G., Reynolds, M. R., Ryan, T. P., and Woodall, W. H. (2000), The State of Statistical Process Control as We Proceed into the 21st Century, *Journal of the American Statistical Association*, **95**(451), 992-998.

Superville, C. R. and Adams, B. M. (1994), An Evaluation of Forecast-Based Quality Control Schemes, *Communications in Statistics: Simulation and Computation*, **23**(3), 645-661.

VanBrackle, L. N. and Reynolds, M. R., Jr. (1997), EWMA and CUSUM Control Charts in the Presence of Correlation, *Communications in Statistics:Simulation and Computation*, **26**(3), 979-1008.

Vander Wiel, S. A. (1996), Monitoring Processes That Wander Using Integrated Moving Average Models, *Technometrics*, **38**(2), 139-151.

Vasilopoulos, A. V. and Stamboulis, A. P. (1978), Modification of Control Chart Limits in the Presence of Data Correlation, *Journal of Quality Technology*, **10**(1), 20-30.

Wardell, D. G., Moskowitz, H., and Plante, R. D. (1992), Control Charts In the Presence of Data Correlation, *Management Science*, **38**(8), 1084-1105.

Wardell, D. G., Moskowitz, H., and Plante, R. D. (1994), Run-Length Distributions of Special-Cause Control Charts for Correlated Observations, *Technometrics*, **36**(1), 3-27.

Woodall, W. H. and Faltin, F. (1993), Autocorrelated Data and SPC, *ASQC Statistics Division Newsletter*, **13**(4), 1821.

Woodall, W. H. and Montgomery, D. C. (1999), Research Issues and Ideas in Statistical Process Control, *Journal of Quality Technology*, **31**(4), 376-386.

Yang J. and Makis V. (1997), On the Performance of Classical Control Charts Applied to Process Residuals, *Computers and Industrial Engineering*, **33**, 121-124.

Yashchin, E. (1993), Performance of CUSUM Control Schemes for Serially Correlated Observation, *Technometrics*, **35**(1), 37-52.

Zhang, N. F. (1998), A Statistical Control Chart for Stationary Process Data, *Technometrics*, **40**(1), 24-38.